Available online at http://scik.org
Commun. Math. Biol. Neurosci. 2015, 2015:22
ISSN: 2052-2541

EVALUATING THE EFFECTS OF PRE-EXPOSURE PROPHYLAXIS ON THE OUTCOMES OF PATIENTS WHO FAILED HIV PREVENTION

QIANG LI[1,2], FURONG LU[3], AIJUN FAN[4,*], KAIFA WANG[1,*]

[1]School of Biomedical Engineering, Third Military Medical University, Chongqing 400038, China

[2]Center for Hypertension and Metabolic Diseases, Department of Hypertension and Endocrinology, Daping Hospital, Third Military Medical University, Chongqing Institute of Hypertension, Chongqing 400042, China

[3]Department of Chemistry, College of Chemistry and Chemical Engineering, Chongqing University, Chongqing 400044, China

[4]Chongqing Academy of Science & Technology, Chongqing 401123, China

Abstract. Pre-exposure prophylaxis (PrEP) has been approved as an effective prevention strategy for HIV infection in high-risk populations. However, little is known about its effects on people who have failed to prevent HIV infection. Based on a proposed mathematical HIV-PrEP model, we examined the effectiveness of different drug responses and PrEP times on patient outcomes. Our result demonstrated a significant interaction between the drug response and patient outcomes. The generalized benefits of PrEP on patient outcomes can be observed in all PrEP groups. The optimal PrEP time might correlate with the clinical pharmacology of the drug. From an epidemiological viewpoint, when the drug response reaches a sufficiently high level, the PrEP strategy can successfully control HIV infection at a population level, even for those people who have failed in preventing HIV infection.

Keywords: HIV infection; Pre-exposure prophylaxis; Mathematical model.

2010 AMS Subject Classification: 92D30.

*Corresponding author

E-mail addresses: aijun71@163.com (A. Fan) kfwang72@163.com (K. Wang)

Received November 10, 2014

1. Introduction

An estimated 2.1 million people are newly infected with HIV, and approximately 1.5 million patients died from AIDS in 2013 [1]. Increased attention has been focused on the daily use of antiretroviral drugs to block the propagation of HIV infection in HIV-uninfected and high-risk populations. This strategy is known as pre-exposure prophylaxis (PrEP). García-Lerma *et al.* provided an overview of the rationale behind PrEP [2]. Several HIV prevention trials have focused on PrEP over the past four years [3-13]. Notably, the World Health Organization (WHO) provided a PrEP guidebook for serodiscordant couples, men, and transgender women who have sex with men [14, 15]. This guidebook recommends regimens that include both tenofovir disoproxil fumarate and emtricitabine (TDF plus FTC) or TDF alone. The US Food and Drug Administration (FDA) has approved the once daily combination of TDF plus FTC as PrEP for HIV-negative individuals at high risk of sexually acquired HIV infection [16].

Although the effects of PrEP on HIV prevention have been shown, less is known about the status of those participants who were unsuccessful at preventing infection. Furthermore, several trials have shown the negative effects of PrEP prevention [5, 9, 12]. Therefore, it is important to question whether the effects of PrEP on HIV prevention benefit patients who are infected despite using preventive measures.

Mathematic models have long been used to study virus dynamics, and some models have been used in PrEP studies to evaluate the effects of PrEP at a population level [17, 18]. Considering the abovementioned problems, we mimicked a total of 20,000 participants using a mathematical HIV-PrEP model. We focused on the benefits of PrEP on patients who failed prevention. Findings from this study have potential implications on determining the benefits of PrEP in HIV infection propagation at a population-level of individuals who fail PrEP prevention.

2. Materials and methods

Antiretroviral drug selection

Among the recommended anti-HIV drugs using in clinical PrEP trials, FTC is a nucleoside reverse transcriptase inhibitor (NRTI), while TDF is classified as a nucleotide-analogue reverse

transcriptase inhibitor (NtRTIs). Both drugs act as competitive inhibitors of the normal substrates needed for HIV reverse transcriptase [3, 19], thereby inhibiting the new infection of HIV-susceptible cells. However, NtRTIs are distinguished from the NRTIs because they require only two (not three) phosphorylation steps to be converted to their active forms [3, 19]. In this respect, TDF might be more efficient at preventing HIV. Considering their similar anti-HIV infection mechanisms, we only considered a daily oral regimen with 300-mg dose of TDF in our simulation.

PK-IDR model

The intracellular drug concentration is directly correlated with the drug efficacy in inhibiting HIV infection; and this efficacy can be directly measured by the drug response level. Patient adherence to the regimen also significantly influences PrEP effects, mainly through the changes in intracellular drug concentration caused by discontinuous treatment. Therefore, in order to give a more precise measurement of the PrEP effects on patient outcomes, it is crucial to determine the actual individual drug response level during PrEP.

We first simulated the TDF concentrations in the peripheral blood (PB) and lymph nodes (LNs) using a classic two-compartment pharmacokinetic (PK) model. Based on the generalized clinical or experimental TDF pharmacological research, the pharmacokinetic parameters were established using a least square method.

Note that TDF requires two phosphorylation steps to be converted to its active form after absorption following oral administration [3, 19]. We then used a PK-IDR coupling model to explore such effects, and the half-life of TDF in the HIV-susceptible cells was used to measure the decay of the response [20]. (*See Appendix Methods for a detailed model description.*)

HIV-PrEP model

Based on the above PK-IDR model and using our previous HIV infection therapy model [21], we constructed a mathematical HIV-PrEP model with the actual pharmacological response to TDF following daily oral administration. We used the same initial values from our previous model for every variable. Because the participants might be infected at different times after PrEP initiation, we explored the pharmacodynamic response of TDF by establishing various

HIV exposure days after PrEP initiation. (*See Appendix Methods for a detailed model description.*)

PrEP strategy evaluation

Using the proposed HIV-PrEP model, we further evaluated the effectiveness of PrEP in improving outcome of patients who became infected while undergoing PrEP. First, we modeled 20000 participants using randomly perturbed model parameters and initial conditions with values varying by 10%. Second, 25% of the participants were grouped as normal controls and did not receive TDF treatment. The so-called PrEP time for the control group was the time lag between the start of PrEP and the onset of viral infection. Third, the remaining participants were randomly assigned to one of three different PrEP groups: a high drug response group (n = 5000), a medium drug response group (n = 5000), and a low drug response group (n = 5000), according to the TDF response of cells in the PB. Finally, for all four groups, the HIV exposure time was randomly assigned to each participant, with time points of 30, 90, 210, 480, 810, 1200, 2400, and 3900 days from the beginning, indicating the length of PrEP treatment; the different time points were assigned equally to each group. To mimic person who got infected while missed HIV test and kept on PrEP in the reality world, which may lead to the delayed initiation of HAART treatment, we assumed that the participants could test positive for HIV no more than six times following the HIV monthly test. The sample distributions under the different conditions are shown in *Appendix Table S1*.

Indicators for PrEP effects evaluation

The T4 cell count in the PB is the main indicator of the clinical stage of HIV infection, which was thereby selected as the primary measure of PrEP effects in our study. Note that apoptosis among uninfected T4 cells, which is a major part of T4 cell depletion, was caused indirectly but, was mainly attributed to infected monocytes/macrophages [22], can influence the progression of the disease by acting as the major cause of T4 cell death and viral production [21]. Therefore, the infected monocyte/macrophage counts were also measured. For the sake of clarity, only the cell counts of these two cell types in the PB are illustrated here.

Statistical analysis

Two different ANOVAs were used to show the pharmacodynamic differences of the three drug intervention groups and the influence of drug response and PrEP time on the benefits of patients' outcomes. One-way ANOVA were performed to compare the differences in the responses to TDF in PB and LNs in the three drug intervention groups. Two-way independent-group ANOVA was established to examine the main effects of the two factors (the drug and PrEP factors) and their interaction effects simultaneously. Tukey's honestly significant difference test or the Games Howell *post-hoc* test was used for multiple comparisons because of equal or unequal variance. The analyses were performed using SPSS (version 13.0) and Excel 2003. A two-sided probability value < 0.05 was considered significant.

3. Results

Pharmacodynamic differences in the three drug intervention groups

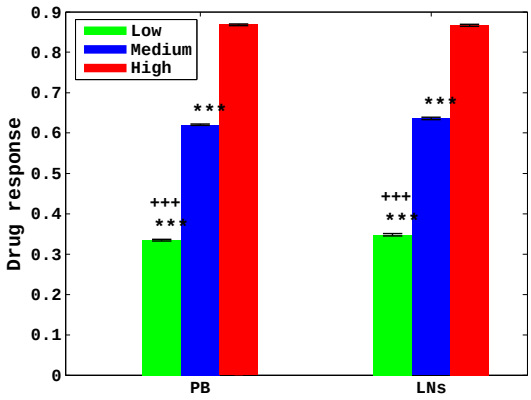

FIGURE 1. Histogram and multiple comparisons of TDF responses in different compartments. The error bars indicate a 95% confidence interval (CI) for each mean (histograms). The asterisk (*) indicates the results of the comparisons with the high drug response group, and the plus sign (+) indicates the results of the comparison between the low and medium drug response groups. Here, *** and +++ denote $P < 0.0001$. PB = peripheral blood; LNs = lymph nodes.

Overall, the drug response levels were different among the groups, as determined using a one-way analysis of variance (ANOVA) ($F(2,14997) = 76273.784, P < 0.0001$ in the peripheral blood [PB] and $F(2,14997) = 33486.468, P < 0.0001$ in the lymph nodes [LNs]). The

Games Howell post-hoc tests revealed that all multiple comparisons demonstrated significant differences (Fig. 1). Fig. 1 also shows that the TDF response increased from the low to high groups. Thus, it is reasonable to divide the three intervention groups by their response levels to TDF.

Influence of drug response and PrEP on immune cells

A significant drug*PrEP interaction was found in both the T4 cell count ($F(21,19968) = 158.994, P < 0.0001, MSe = 56863.334$) and the infected monocyte/macrophage counts ($F(21, 19968) = 103.267, P < 0.0001, MSe = 1090.756$). The simple main effect analyses showed no significant differences for the drug factor within the first PrEP level (30 days) in the T4 cell count ($F(3,19968) = 0.242, P = 0.867, MSe = 56863.334$). Note that Table 1 shows that all other simple main effects were significant either for the drug factor within the other PrEP levels or for the PrEP factor within the different drug levels. Thus, to determine the influence of the drug response and PrEP times on the benefits of immune cells, post-hoc tests were needed to make multiple comparisons of the different drug response or PrEP time levels. Fig. 2 shows the histogram and part of the multiple comparison analysis of the T4 cell and infected monocyte/macrophage cell counts following different drug response and PrEP time levels.

TABLE *1. Results of the independent-group two-way ANOVAs and simple main effects.*

Index	**Source**	**df**	**Mean Square**	**F**	**Sig.**
T4 cell count in PB	Drug	3	231771253.842	4075.935	0.000
	PrEP	7	14797676.447	260.232	0.000
	Drug*PrEP	21	9040907.683	158.994	0.000
	Drug Within PrEP(1)	3	13745.277	0.242	0.867
	Drug Within PrEP(2)	3	3689534.446	64.884	0.000
	Drug Within PrEP(3)	3	37261056.171	655.274	0.000
	Drug Within PrEP(4)	3	58482916.874	1028.482	0.000
	Drug Within PrEP(5)	3	62427362.902	1097.849	0.000
	Drug Within PrEP(6)	3	57511868.375	1011.405	0.000
	Drug Within PrEP(7)	3	50366326.388	885.743	0.000
	Drug Within PrEP(8)	3	25304797.190	445.011	0.000
	PrEP Within Drug(1)	7	35263192.025	620.139	0.000
	PrEP Within Drug(2)	7	5901395.162	103.782	0.000
	PrEP Within Drug(3)	7	380445.766	6.691	0.000
	PrEP Within Drug(4)	7	375366.543	6.601	0.000
	Error	19968	56863.334		

TABLE *1. (Continue)*

Index	Source	df	Mean Square	F	Sig.
Infected	Drug	3	2074531.398	1,901.920	0.000
monocytes/macrophages	PrEP	7	400446.399	367.127	0.000
count in PB	Drug*PrEP	21	112638.653	103.267	0.000
	Drug Within PrEP(1)	3	22790.904	20.895	0.000
	Drug Within PrEP(2)	3	45512.570	41.726	0.000
	Drug Within PrEP(3)	3	122579.305	112.380	0.000
	Drug Within PrEP(4)	3	175803.988	161.176	0.000
	Drug Within PrEP(5)	3	217533.168	199.433	0.000
	Drug Within PrEP(6)	3	259450.200	237.863	0.000
	Drug Within PrEP(7)	3	659606.895	604.724	0.000
	Drug Within PrEP(8)	3	1359724.940	1246.589	0.000
	PrEP Within Drug(1)	7	7521.506	6.896	0.000
	PrEP Within Drug(2)	7	21951.497	20.125	0.000
	PrEP Within Drug(3)	7	155681.270	142.728	0.000
	PrEP Within Drug(4)	7	553208.086	507.178	0.000
	Error	19968	1090.756		

Effectiveness of drug response

To show the effectiveness of the drug response and find the optimal drug response based on the different PrEP times, we focused on the comparisons between the high response group and the normal group, between the medium response group and the normal group, and between the low response group and the normal group.

After 30 days of PrEP, the high and medium drug response group had an increased T4 cell count compared to the normal control group, as shown in Fig. 2A. However, there was no difference between the low drug response group and the normal control group when the PrEP time was more than 810 days. In contrast, the infected monocyte/macrophage counts decreased in all drug response groups (compared to the normal group) at all PrEP time levels, as shown in Fig. 2B.

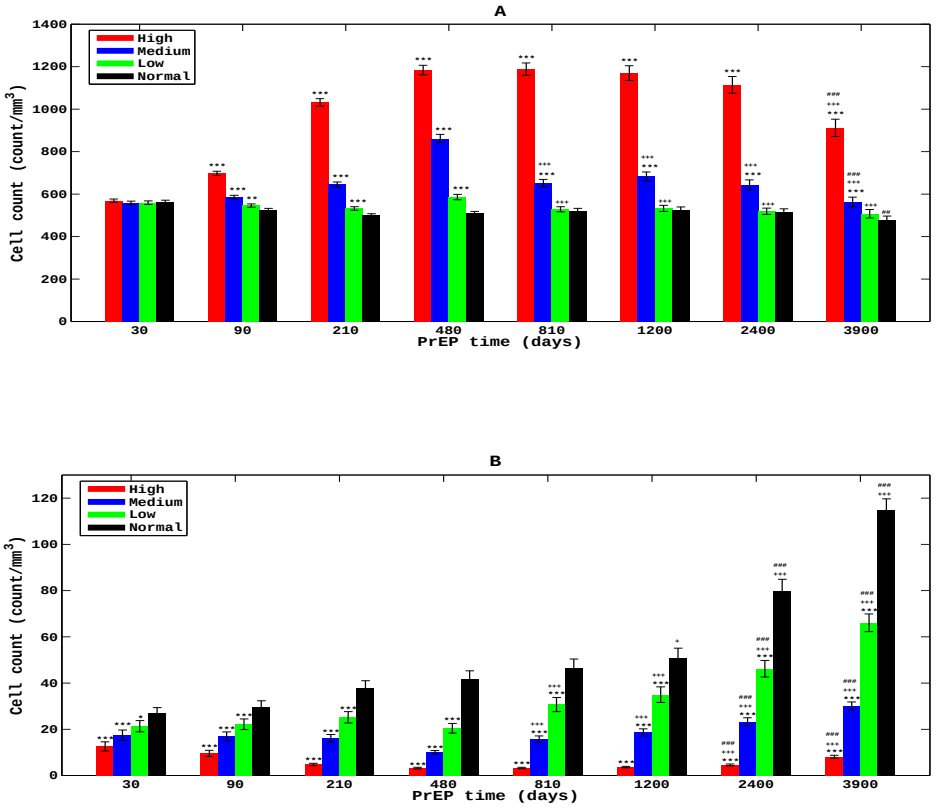

FIGURE 2. Histogram and part of the multiple comparisons analysis for the detection indices following different drug responses and PrEP times. The error bars indicate a 95% CI for each mean (histograms). (A) T4 cell counts in the PB and (B) infected monocyte/macrophage counts in the PB. The asterisk (*) indicates the results of the comparisons with the normal group under different PrEP times. The plus sign (+) indicates the results of the comparisons between PrEP times of 480 days and other PrEP times with the different drug responses, and the pound sign (♯) indicates the results of the comparisons between PrEP times of 810 days and other PrEP times with the different drug responses. Here, *, +, and ♯ denote $P < 0.05$, whereas **, ++, and ♯♯ denote $P < 0.01$, and ***, +++, and ♯♯♯ denote $P < 0.0001$. High = high drug response group; Medium = medium drug response group; Low = low drug response group; Normal = normal control group.

Note that higher T4 cell counts and lower infected monocyte/macrophage counts indicate a better patient prognosis. Thus, despite the fact that there are some slight but balanced differences in these two indices, all drug efficacies could induce a better prognosis, particularly within the high and medium drug response groups.

Moreover, note that the T4 cell count was > 900 cells/mm^3 in the high drug response group when the PrEP time was greater than 210 days (Fig. 2A). Because the case reproduction number is currently less than one [23], we suggested from an epidemiological perspective that when the TDF response reaches a sufficiently high level, the PrEP strategy can successfully control HIV infection at a population level, even for those people who have failed in preventing HIV infection. The area-fill graph also visually reflects the comparison of T4 cell counts between the high drug response group and all three PrEP groups (Fig. 3).

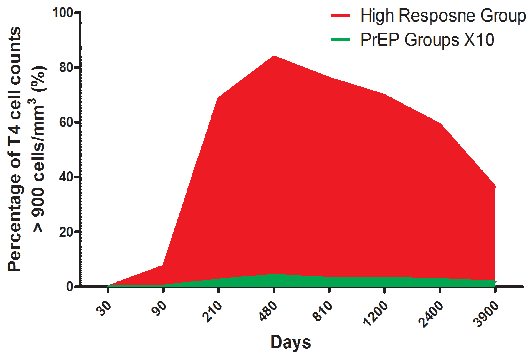

FIGURE 3. Area-fill graph illustrates the comparison of T4 cell counts between the high drug response group and all three PrEP groups. The percentage of the high drug response group was calculated by dividing the total participant counts in each PrEP time (n = 625) by those participants whose T4 cell counts were > 900 cells/mm^3. To calculate the percentage in all three PrEP groups, the total number of participants from the three PrEP groups with T4 cell counts > 900 cells/mm^3 was divided by the total number of participants in all three PrEP groups under each PrEP time (n = 1875). Notably, the percentages calculated for the total of the three PrEP groups were multiplied by 10 to be drawn at the same scale of the percentages from the high drug response group.

Effectiveness of PrEP time

According to Fig. 2, when the drug response is high, we found that the top two T4 cell counts and the lowest two infected monocyte/macrophage counts occurred at the fourth level (480 days) and fifth level (810 days) of the PrEP time factor, and there was no significant difference between them. Therefore, we focused on comparing the longer levels of the PrEP factor to the fourth level or fifth level under different drug responses. The goal of this study was to show the effectiveness of PrEP time on patients' outcomes.

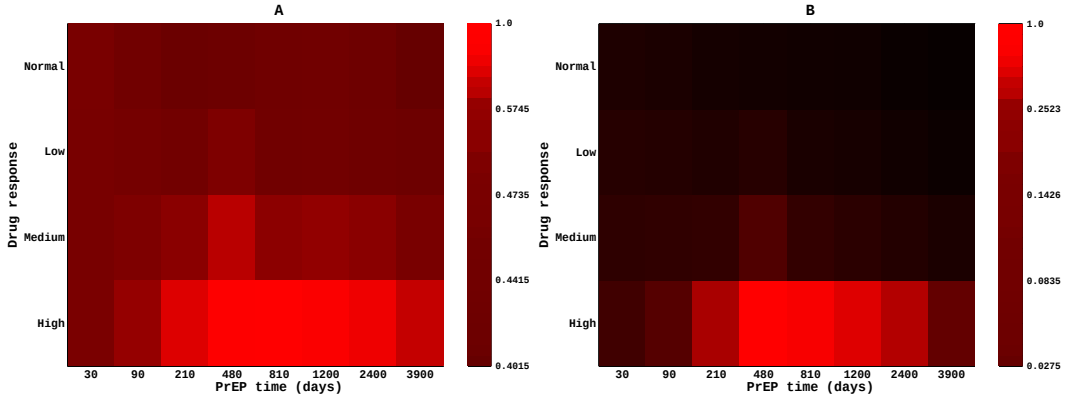

FIGURE 4. Color-coded boxes reflect the influence of the drug response and PrEP time on HIV infection. (A) T4 cell count in the PB and (B) infected monocyte/macrophage count in the PB. First, we determined the maximum (minimum) mean of the T4 cell (infected monocyte/macrophage) counts among all 32 situations (i.e., four different drug responses and eight different PrEP times) in our theoretical clinical trial. Then, for each mean of the T4 cell counts, we divided by the maximum mean of the T4 cell counts. Concurrently, for the minimum mean of the infected monocyte/macrophage counts, we divided by each mean of the infected monocyte/macrophage counts. Finally, for each small box, we set the corresponding quotient as the amount of the red component and set the green and blue components to zero. Note that higher T4 cell counts and lower infected monocyte/macrophage counts indicate a better patient prognosis. Thus, deeper red components indicate a better prognosis, and the pure red component corresponds to the best prognosis. High = high drug response group; Medium = medium drug response group; Low = low drug response group; and Normal = normal control group.

By comparing the typical cell counts at 480 days or 810 days with those from longer PrEP times, we obtained the following results. For the T4 cell count index, when the drug response was high, there was no difference except when comparing 480 days of PrEP time with 3900 days of PrEP time. When the drug response was medium or low, the differences were centered on comparisons between 480 days and the other longer PrEP times. For the infected monocyte/macrophage count index, the cell counts for 480 days or 810 days of PrEP treatment were significantly lower than the other longer PrEP times in nearly all drug response groups. These results convinced us that a PrEP time of 480 days may be sufficient to obtain a higher T4 cell count and a lower infected monocyte/macrophage count.

According to the overall size of the indices and the significance of the multiple comparisons, we can conclude that the PrEP strategy benefits individuals who infected HIV during prevention, and it helps them obtain a more favorable prognosis. The optimal PrEP time may be between 480 and 810 days, i.e, PrEP for this length of time can lead to better prognosis. To intuitively demonstrate these results, a color-coded box was designed to reflect the influence of the drug response and PrEP time (Fig. 4), and this graph visually confirmed our previous results.

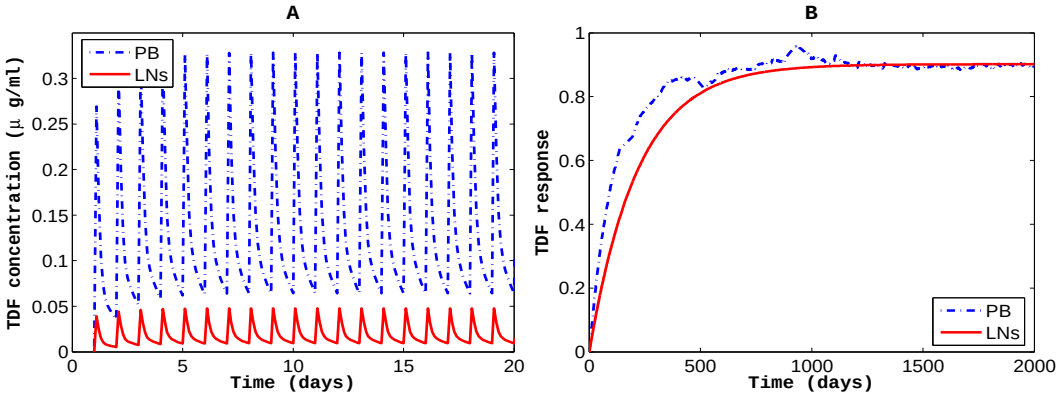

FIGURE 5. Simulated drug concentrations and responses in both compartments. The parameter values are the same as that shown in *Appendix Table S2*. Here, we simulated only a high drug response, and the values selected for E_{max}^{PB} and E_{max}^{LNs} were 0.05257 and 0.015, respectively. The TDF plasma concentration correlated well with the clinical data. Although they had the same TDF response, we can see that the times to reach the maximum response are different between the PB and LNs.

Using the estimated parameter values shown in *Appendix Table S3*, Fig. 5 illustrates the simulated drug concentrations and responses in both compartments. We found that the estimated TDF concentration change after periodic administration correlated well with the features (Fig. 5A). Approximately 800 days after the TDF tablet was taken, the drug response in the blood and lymph nodes achieved stable levels, although there are some differences in their patterns (Fig. 5B). Of notably, our result suggests that the optimal PrEP treatment time might correlate with clinical pharmacology, since the preventive treatment times closest to achieving the maximum drug response level.

4. Discussion and conclusions

PrEP strategy had shown effectiveness in preventing HIV infection. However, little attention has been focused on its effects in individuals who infected HIV while undergoing preventive treatment. A new mathematical HIV-PrEP model has been proposed, in which combines a classic PK-IDR model and our previous HIV infection therapy model [21]. Based on this model, 20000 participants with a maximum prevention time > 10 years were mimicked. Our study suggests that the PrEP strategy could benefit people who become infected during prevention. In particular, at a population level using PrEP strategy, the patients who exhibit a high drug response may control HIV infection propagation.

From an epidemiological standpoint, Granich et al. suggested that individuals should begin highly active antiretroviral therapy (HAART) when their T4 cell counts in the PB are > 900 cells/mm^3; this therapy would ensure that the disease does not become prevalent at a population level [23]. Our results show that the effects of PrEP on patients can be seriously affected by the patient's response to the drug. An evaluation of diverse drug responses shows that the PrEP strategy can successfully control HIV infection when the TDF response reaches a sufficiently high level. Even for the remaining patients, PrEP strategy could still lead to a better prognosis. Additionally, we found that the amount of infected monocyte/macrophage decreases significantly when patients undergo PrEP, regardless of the drug response. This result further confirms our previous statement that the number of infected monocytes/macrophages correlates with disease progression and might be used as an alternative monitor of HIV infection [21].

Notably, Anderson et al. determined the drug concentrations that are associated with protecting individuals from acquiring HIV-1 infection [13]. The authors concluded that an intracellular concentration of 16 fmol of the active form of tenofovir per 10^6 peripheral blood mononuclear cells (PBMCs) was associated with a 90% reduction in HIV acquisition [13]. The intracellular drug concentration is directly correlated with the efficiency of the drug in inhibiting HIV infection and can be expressed as the drug response levels. Our study further showed that the effects of PrEP on improved patient outcomes could also be influenced by the drug concentration.

The estimated optimal prevention time points occur between 480 and 810 days, which is the time closest to achieving the maximum drug response level. Thus, the optimal PrEP treatment time might correlate with clinical pharmacology. The occurrence of optimal time points suggests that strict adherence to the drug regimen and long-term prevention strategies are important. As our study demonstrated, even patients infected during prevention can still obtain better outcomes under these conditions.

Our model allows us to take a global view and comprehensively consider how the immune system responds to the HIV virus and how a patient's response to TDF may change. In the future, the focus of constructing mathematical models should based on more detailed biological mechanisms and that consider more aspects of the PrEP strategy, such as FTC administration and sexual differences.

Appendix

TABLE *S1. Sample sizes under different design conditions in our theoretical clinical trial.*

Drug	**PrEP time**							
response	30 d	90 d	210 d	480 d	810 d	1200 d	2400 d	3900 d
High	625	625	625	625	625	625	625	625
Medium	625	625	625	625	625	625	625	625
Low	625	625	625	625	625	625	625	625
Normal	625	625	625	625	625	625	625	625

Methods

PK-IDR model

PK model of a single oral TDF administration

The classic two-compartment pharmacokinetic (PK) model with a single extravascular administration can be described by the following three differential equations:

$$\begin{cases} \frac{dD_a}{dt} = -K_a D_a, \\ \frac{dD_c}{dt} = K_a D_a - (K_{12} + K_e) D_c + K_{21} D_p, \\ \frac{dD_p}{dt} = K_{12} D_c - K_{21} D_p. \end{cases} \tag{1}$$

where D_a, D_c and D_p represent the drug dosage at time t in absorption (e.g., stomach), central (e.g., PB), and peripheral (e.g., LNs) compartments, respectively. The parameters K_a, K_{12} and K_{21} are the transfer rate constants between each compartment, and K_e denotes the elimination rate constant of the central compartment. The analytic solution of the equations (1) is as follows:

$$\begin{cases} D_a = D_0 e^{-K_a t}, \\ D_c = B_1 e^{-\alpha t} + B_2 e^{-\beta t} - (B_1 + B_2) e^{-K_a t}, \\ D_p = \frac{\beta - K_{21}}{K_{21}} B_1 e^{-\alpha t} + \frac{\alpha - K_{21}}{K_{21}} B_2 e^{-\beta t} - (\frac{\beta - K_{21}}{K_{21}} B_1 + \frac{\alpha - K_{21}}{K_{21}} B_2) e^{-K_a t}, \end{cases} \tag{2}$$

in which D_0 is the initial drug dosage, and

$$\begin{aligned} &B_1 = \frac{(K_{21} - \alpha) K_a}{(\beta - \alpha)(K_a - \alpha)} D_0, \qquad B_2 = \frac{(K_{21} - \beta) K_a}{(\alpha - \beta)(K_a - \beta)} D_0, \\ &\alpha + \beta = K_{12} + K_{21} + K_e, \quad \alpha\beta = K_{21} K_e. \end{aligned} \tag{3}$$

PK model of periodic oral TDF administration

We assumed the interval between the two administrations was τ, with a dosage of D_0, and a bioavailability of F. Therefore, after the second TDF administration of time t ($0 \leq t \leq \tau$), the drug dose in the central compartment can be formulated using the following equation:

$$D_c^{(2)}(t) = B_1 (e^{-\alpha\tau} + 1) e^{-\alpha t} + B_2 (e^{-\beta\tau} + 1) e^{-\beta t} - (B_1 + B_2)(e^{-K_a\tau} + 1) e^{-K_a t}. \tag{4}$$

Note that time t in equation (4) is the renew time following the second administration. Therefore, the drug dose in the central compartment at time t after n times of TDF administration is

as follows:

$$\begin{aligned} D_c^{(n)}(t) &= B_1(e^{-(n-1)\alpha\tau}+e^{-(n-2)\alpha\tau}+\cdots+e^{-\alpha\tau}+1)e^{-\alpha t} \\ &\quad +B_2(e^{-(n-1)\beta\tau}+e^{-(n-2)\beta\tau}+\cdots+e^{-\beta\tau}+1)e^{-\beta t} \\ &\quad -(B_1+B_2)(e^{-(n-1)K_a\tau}+e^{-(n-2)K_a\tau}+\cdots+e^{-K_a\tau}+1)e^{-K_a t} \\ &= B_1\tfrac{1-e^{n\alpha\tau}}{1-e^{-\alpha\tau}}e^{-\alpha t}+B_2\tfrac{1-e^{n\beta\tau}}{1-e^{-\beta\tau}}e^{-\beta t}-(B_1+B_2)\tfrac{1-e^{nK_a\tau}}{1-e^{-K_a\tau}}e^{-K_a t}. \end{aligned} \tag{5}$$

Dividing the above equation by the apparent volume of distribution of the PB, V_1, we obtained the drug concentration expression in the PB as follows:

$$C_c^{(n)}(t)=A_{1c}\frac{1-e^{n\alpha\tau}}{1-e^{-\alpha\tau}}e^{-\alpha t}+A_{2c}\frac{1-e^{n\beta\tau}}{1-e^{-\beta\tau}}e^{-\beta t}-(A_{1c}+A_{2c})\frac{1-e^{nK_a\tau}}{1-e^{-K_a\tau}}e^{-K_a t}. \tag{6}$$

in which $A_{1c}=B_1/V_1$ and $A_{2c}=B_2/V_1$.

Similarly, the drug concentration expression in the LNs with periodic oral TDF administration can be formulated using the following equation:

$$\begin{aligned} C_p^{(n)}(t) =& \frac{\beta-K_{21}}{K_{21}}A_{1p}\frac{1-e^{n\alpha\tau}}{1-e^{-\alpha\tau}}e^{-\alpha t}+\frac{\alpha-K_{21}}{K_{21}}A_{2p}\frac{1-e^{n\beta\tau}}{1-e^{-\beta\tau}}e^{-\beta t} \\ & -(\frac{\beta-K_{21}}{K_{21}}A_{1p}+\frac{\alpha-K_{21}}{K_{21}}A_{2p})\frac{1-e^{nK_a\tau}}{1-e^{-K_a\tau}}e^{-K_a t}. \end{aligned} \tag{7}$$

in which $A_{1p}=B_1/V_2, A_{2p}=B_2/V_2$ and V_2 is the apparent volume of the distribution of the LNs.

PK model coupled with an IDR model

Indirect pharmacodynamic response (IDR) models have been proposed to characterize the drug pharmacodynamics that produce responses after a time lag or act by indirect mechanisms [22]. We assumed here that intracellular accumulation of TDF was obtained by stimulation of K_{in} from the plasma TDF concentration. Therefore, the TDF plasma concentration increases intracellular TDF deposition through an indirect response, which can be expressed as

$$\frac{dR}{dt}=K_{in}(1+\frac{E_{max}C}{SC_{50}+C})-K_{out}R. \tag{8}$$

where R is a measured response to TDF by indirect mechanisms, C is the TDF concentration in the PB or LNs, K_{in} represents the zero-order constant for the production of the response, and K_{out} defines the first-order rate constant for the loss of the response. E_{max} represents the

coefficient of the drug response level, and SC_{50} represents the TDF plasma concentration that produces 50% of the intracellular response.

Parameter estimation

Based on the known pharmacokinetic and pharmacodynamic parameters (Table S2) and using the following parameter estimation equations (9) and the least square method, we can estimate the key parameters of equations (6) and (7), which are shown in Table S3.

TABLE *S2. The known pharmacokinetic and pharmacodynamic parameters and their values.*

Parameter	Definitions	Value	Reference
C_{max}	Maximum serum drug concentration	0.3 μg/ml	24,25
C_{min}	Minimum serum drug concentration	0.0644 μg/ml	26
AUC	Area under the curve	3.324 μg.h/ml	26
$T_{1/2,plasma}$	Half elimination rate in plasma	17 h	24
F	Bioavailability	25%	25,26
D_0	Dosage	300 mg	27
τ	Interval between administrations of TDF	24 h	27
T_m	Time to reach C_{max}	1 h	24,25
V_d	Total volume of distribution at steady-state	0.8 L/kg	26
K_{in}^{PB}	Zero-order constant of response production in plasma cells	0.276	28
K_{in}^{LNs}	Zero-order constant of response production in lymph node cells	0.276	28
K_{out}^{PB}	First-order rate of response loss in plasma cells	0.0087	28,29
K_{out}^{LNs}	First-order rate of response loss in lymph node cells	0.0046	29
SC_{50}^{PB}	TDF plasma concentration producing 50% of the intracellular response	0.1	28
SC_{50}^{LNs}	TDF lymph node concentration producing 50% of the intracellular response	0.001	28

Note that the above equations are all derived from the steady-state plasma drug concentrations. For the estimation of parameter β, we used the equation $CL = D_0F/AUC = \beta V_d$. To mimic three levels for the coefficient of the drug response levels, we used sequential search arithmetic and estimated three values each for the plasma and lymph nodes (0.05257/0.0355/0.0177 and 0.015/0.01/0.005, respectively) (Table S3). The calculated drug responses under each circumstance of those values are 0.9/0.9, 0.6/0.6 and 0.3/0.3 for each compartment. We defined those drug responses as high, medium, and low, which could be altered by a random perturbation technique. In our theoretical clinical trial, we set three degrees of TDF responses in cells: high ($R \geq 0.75$), medium ($0.5 \leq R < 0.75$), and low ($R < 0.5$), as measured by the magnitude of the response in the plasma. The variable effectiveness of the drug responses characterized different participants' reaction to TDF intake.

$$\begin{cases} C_{max} = \frac{A_{1c}e^{-\alpha T_m}}{1-e^{-\alpha\tau}} + \frac{A_{2c}e^{-\beta T_m}}{1-e^{-\beta\tau}} - \frac{(A_{1c}+A_{2c})e^{-K_a T_m}}{1-e^{-K_a\tau}}, \\ C_{min} = \frac{A_{1c}}{1-e^{-\alpha\tau}} + \frac{A_{2c}}{1-e^{-\beta\tau}} - \frac{A_{1c}+A_{2c}}{1-e^{-K_a\tau}}, \\ AUC = \frac{A_{1c}}{\alpha} + \frac{A_{2c}}{\beta} - \frac{A_{1c}+A_{2c}}{K_a}, \\ CL = \frac{\alpha\beta V_1}{K_{21}}. \end{cases} \tag{9}$$

TABLE *S3. The estimated parameter values of the PK-IDR model.*

Parameter	Definitions	Value
α	Half distribution rate in plasma	0.7313
β	Half elimination rate in plasma	0.4701
K_{21}	Transportation rate constant from LN to PB	0.0927
K_a	Transportation rate constant of absorption to PB	0.0339
V_1	Volume of distribution at steady-state in PB	6.0858 L
V_2	Volume of distribution at steady-state in LN	41.9142 L
E_{max}^{PB}	Coefficient of drug response level in plasma	0.05257/0.0355/0.0177
E_{max}^{LNs}	Coefficient of drug response level in lymph nodes	0.015/0.01/0.005

HIV-PrEP model

In our previous HIV infection therapy model [20], we used both reverse transcriptase inhibitors (RTIs) and protease inhibitors (PIs). Here, we eliminated the PI effects and changed the constant RTI response in our PK-IDR model. Additionally, we assumed no differences in

drug effectiveness between the monocytes/macrophages and lymphocytes. In addition to the traditional equations (10)-(44), equations (45) and (46) were added to describe the intracellular TDF accumulation in the PB and LN, respectively. A comprehensive survey of our previous HIV infection therapy model and its variables, parameter values, initial values, and relations to our PK-IDR model are described elsewhere [20]. The complete HIV infection PrEP model is listed below.

Equations (10)-(17) represent the dynamic behaviors of T4 cells in the PB, including the HIV-specific and -nonspecific T4 cells. Note that TDF is an NtRTIs and inhibits cell infection and therefore diminishes the part of infected cell generation in the corresponding equation. Because we have determined the drug effectiveness in equations (45) and (46), we represent the inhibition effects of TDF using $(1-R_{PB}^{RT})$ and $(1-R_{LN}^{RT})$. The subscript "PB" or "LN" denotes that the corresponding drug effectiveness is measured in the PB or the LNs.

$$\begin{aligned}\frac{d\tilde{T}_{PB,4n}}{dt} =& vf(1-\frac{eV_{PB}}{c_1+V_{PB}})s+\frac{V_{PB}}{c_2+V_{PB}}(1-\varphi)\rho_{4n}\tilde{T}_{PB,4n}-k_V(1-R_{PB}^{RT})\frac{V_{PB}}{c_2+V_{PB}}\tilde{T}_{PB,4n}\\ &-\mu_{4n}\tilde{T}_{PB,4n}-0.1(1-P_{Inf}^{PB})\mu_{4n}M_o^i\tilde{T}_{PB,4n}-0.1P_{Inf}^{PB}(1-R_{PB}^{RT})\delta M_o^i\tilde{T}_{PB,4n},\end{aligned} \tag{10}$$

$$\frac{d\tilde{T}_{PB,4e}}{dt} =\frac{V_{PB}}{c_2+V_{PB}}\varphi\rho_{4n}\tilde{T}_{PB,4n}-k_V(1-R_{PB}^{RT})\frac{V_{PB}}{c_2+V_{PB}}\tilde{T}_{PB,4e}-\mu_{4e}\tilde{T}_{PB,4e}, \tag{11}$$

$$\begin{aligned}\frac{d\tilde{T}_{PB,4n}^i}{dt} =& vf(1-\frac{eV_{PB}}{c_1+V_{PB}})s+(1-\varphi)(1-p)\frac{V_{PB}}{c_2+V_{PB}}\rho_{4n}\tilde{T}_{PB,4n}^i+k_V(1-R_{PB}^{RT})\\ &\frac{V_{PB}}{c_2+V_{PB}}\tilde{T}_{PB,4n}-(k_8\delta\tilde{T}_{PB,8e}+\mu_{4n}^i)\tilde{T}_{PB,4n}^i+0.1P_{Inf}^{PB}(1-R_{PB}^{RT})\delta M_o^i\tilde{T}_{PB,4n},\end{aligned} \tag{12}$$

$$\begin{aligned}\frac{d\tilde{T}_{PB,4e}^i}{dt} =&\varphi(1-p)\frac{V_{PB}}{c_2+V_{PB}}\rho_{4n}\tilde{T}_{PB,4n}^i+k_V(1-R_{PB}^{RT})\frac{V_{PB}}{c_2+V_{PB}}\tilde{T}_{PB,4e}\\ &-(k_8\tilde{T}_{PB,8e}+\mu_{4e}^i)\tilde{T}_{PB,4e}^i,\end{aligned} \tag{13}$$

$$\begin{aligned}\frac{dT_{PB,4n}}{dt} =&(1-v)f(1-\frac{eV_{PB}}{c_1+V_{PB}})s+(1-\varphi)\gamma_4T_{PB,4n}-k_V(1-R_{PB}^{RT})\frac{V_{PB}}{c_2+V_{PB}}T_{PB,4n}\\ &-\mu_{4n}T_{PB,4n}-0.1\mu_{4n}M_o^iT_{PB,4n},\end{aligned} \tag{14}$$

$$\frac{dT_{PB,4e}}{dt} =\varphi\gamma_4T_{PB,4n}-k_V(1-R_{PB}^{RT})\frac{V_{PB}}{c_2+V_{PB}}T_{PB,4e}-\mu_{4e}T_{PB,4e}, \tag{15}$$

$$\begin{aligned}\frac{dT_{PB,4n}^i}{dt} =&(1-v)f(1-\frac{eV_{PB}}{c_1+V_{PB}})s+(1-\varphi)(1-p)\gamma_4T_{PB,4n}^i\\ &+k_V(1-R_{PB}^{RT})\frac{V_{PB}}{c_2+V_{PB}}T_{PB,4n}-(k_8\delta\tilde{T}_{PB,8e}+\mu_{4n}^i)T_{PB,4n}^i,\end{aligned} \tag{16}$$

$$\frac{dT^i_{PB,4e}}{dt} = \varphi(1-p)\gamma_4 T^i_{PB,4n} + k_V(1-R^{RT}_{PB})\frac{V_{PB}}{c_2+V_{PB}}T_{PB,4e} - (k_8\tilde{T}_{PB,8e} + \mu^i_{4e})T^i_{PB,4e}. \tag{17}$$

Equations (18)-(21) model the dynamics of T8 cells. Because T8 cells are not the target cells of HIV infection, no drug effects are considered here.

$$\frac{d\tilde{T}_{PB,8n}}{dt} = v(1-f)s + (1-\varphi)R\tilde{T}_{PB,8n} - \mu_{8n}\tilde{T}_{PB,8n}, \tag{18}$$

$$\frac{d\tilde{T}_{PB,8e}}{dt} = \varphi R\tilde{T}_{PB,8n} - \mu_{8e}\tilde{T}_{PB,8e}, \tag{19}$$

$$\frac{dT_{PB,8n}}{dt} = (1-v)(1-f)s + (1-\varphi)\gamma_8 T_{PB,8n} - \mu_{8n}T_{PB,8n}, \tag{20}$$

$$\frac{dT_{PB,8e}}{dt} = \varphi\gamma_8 T_{PB,8n} - \mu_{8e}\tilde{T}_{PB,8e}. \tag{21}$$

Equations (22) and (23) show the dynamics of the actively infected T4 cells and B cells that produce HIV-1 specific antibodies. Actively infected T4 cells that produce free viral particles are generated from latently infected T4 cells.

$$\frac{dT_{PB,i}}{dt} = p(\gamma_4 T^i_{PB,4n} + \rho_{4n}\frac{V_{PB}}{c_2+V_{PB}}\tilde{T}^i_{PB,4n}) - (k_8\tilde{T}_{PB,8e} + \mu_1)T_{PB,i}, \tag{22}$$

$$\frac{dS_{PB,Ab}}{dt} = p\rho_{Ab}(\tilde{T}^i_{PB,4e} + \tilde{T}_{PB,4e})\frac{V_{PB}}{c_2+V_{PB}} - k_{Ab}V_{PB}S_{PB,Ab} - \mu_{Ab}S_{PB,Ab}. \tag{23}$$

Equations (24) and (25) model the dynamics of the activated and infected monocytes in the PB. Note that the third term represents the cell migration from the PB to the LNs and CNS.

$$\frac{dM^a_o}{dt} = \frac{V_{PB}}{c_2+V_{PB}}(M_o - M^i_o - M^a_o) - \mu^a_{Mo}M^a_o - (P_{LN}+P_{CNS})M^a_o, \tag{24}$$

$$\frac{dM^i_o}{dt} = k_{V,M_o}(1-R^{RT}_{PB})\frac{V_{PB}}{c_2+V_{PB}}(M_o - M^i_o) - \mu^i_{Mo}M^i_o - (P_{LN}+P_{CNS})M^i_o - k_8\delta\tilde{T}_{PB,8e}M^i_o. \tag{25}$$

Free virus dynamics are represented in equation (26), with the consideration of viral transition between the PB and LNs.

$$\begin{aligned}\frac{dV_{PB}}{dt} =& N_M M^i_o + N_T(\mu_i T_{PB,i} + \mu^i_{4e}\tilde{T}^i_{PB,4e} + \mu^i_{4e}T^i_{PB,4e}) - k_m\frac{V_{PB}}{c_2+V_{PB}}M^a_o - \frac{eV_{PB}}{c_1+V_{PB}}s \\ &- k_{V,M_o}(1-R^{RT}_{PB})\frac{V_{PB}}{c_2+V_{PB}}(M_o - M^i_o) - \mu_V V_{PB} - R^V_{PB\to LV}V_{PB} + R^V_{LN\to PB}V_{LN} \\ &- k_V(1-R^{RT}_{PB})\frac{V_{PB}}{c_2+V_{PB}}(\tilde{T}_{PB,4n} + \tilde{T}_{PB,4e} + T_{PB,4n} + T_{PB,4e}) - k_{Ab}V_{PB}S_{PB,Ab}.\end{aligned} \tag{26}$$

The fundamental immune response in the LNs is similar to that in the PB. However, a new cell type, FDCs, is added here due to their special location in the LNs. Concretely, equation (44) represents the dynamics of the FDCs.

$$\begin{aligned}\frac{d\tilde{T}_{LN,4n}}{dt} =& vf(1-\frac{eV_{LN}}{c_1+V_{LN}})s+\frac{V_{LN}}{c_2+V_{LN}}(1-\varphi)\rho_{4n}\tilde{T}_{LN,4n}\\ &-k_V(1-R_{LN}^{RT})\frac{V_{LN}}{c_2+V_{LN}}\tilde{T}_{LN,4n}-\mu_{4n}\tilde{T}_{LN,4n}-C_{T4}^{Mi}(1-P_{Inf}^{LN})\mu_{4n}M^i\tilde{T}_{LN,4n}\\ &-P_{Inf}^{LN}(1-R_{LN}^{RT})\delta(M^i+FDC^i)\tilde{T}_{LN,4n},\end{aligned} \tag{27}$$

$$\frac{d\tilde{T}_{LN,4e}}{dt} =\frac{V_{LN}}{c_2+V_{LN}}\varphi\rho_{4n}\tilde{T}_{LN,4n}-k_V(1-R_{LN}^{RT})\frac{V_{LN}}{c_2+V_{LN}}\tilde{T}_{LN,4e}-\mu_{4e}\tilde{T}_{LN,4e}, \tag{28}$$

$$\begin{aligned}\frac{d\tilde{T}_{LN,4n}^i}{dt} =& vf(1-\frac{eV_{LN}}{c_1+V_{LN}})s+(1-\varphi)(1-p)\frac{V_{LN}}{c_2+V_{LN}}\rho_{4n}\tilde{T}_{LN,4n}^i\\ &+k_V(1-R_{LN}^{RT})\frac{V_{LN}}{c_2+V_{LN}}\tilde{T}_{LN,4n}-(k_8\delta\tilde{T}_{LN,8e}+\mu_{4n}^i)\tilde{T}_{LN,4n}^i\\ &+P_{Inf}^{LN}(1-R_{LN}^{RT})\delta(M^i+FDC^i)\tilde{T}_{LN,4n},\end{aligned} \tag{29}$$

$$\begin{aligned}\frac{d\tilde{T}_{LN,4e}^i}{dt} =&\varphi(1-p)\frac{V_{LN}}{c_2+V_{LN}}\rho_{4n}\tilde{T}_{LN,4n}^i+k_V(1-R_{LN}^{RT})\frac{V_{LN}}{c_2+V_{LN}}\tilde{T}_{LN,4e}\\ &-(k_8\tilde{T}_{LN,8e}+\mu_{4e}^i)\tilde{T}_{LN,4e}^i,\end{aligned} \tag{30}$$

$$\begin{aligned}\frac{dT_{LN,4n}}{dt} =&(1-v)f(1-\frac{eV_{LN}}{c_1+V_{LN}})s+(1-\varphi)\gamma_4T_{LN,4n}-k_V(1-R_{LN}^{RT})\frac{V_{LN}}{c_2+V_{LN}}T_{LN,4n}\\ &-\mu_{4n}T_{LN,4n}-C_{T4}^{Mi}\mu_{4n}M^iT_{LN,4n},\end{aligned} \tag{31}$$

$$\frac{dT_{LN,4e}}{dt} =\varphi\gamma_4T_{LN,4n}-k_V(1-R_{LN}^{RT})\frac{V_{LN}}{c_2+V_{LN}}T_{LN,4e}-\mu_{4e}T_{LN,4e}, \tag{32}$$

$$\begin{aligned}\frac{dT_{LN,4n}^i}{dt} =&(1-v)f(1-\frac{eV_{LN}}{c_1+V_{LN}})s+(1-\varphi)(1-p)\gamma_4T_{LN,4n}^i\\ &+k_V(1-R_{LN}^{RT})\frac{V_{LN}}{c_2+V_{LN}}T_{LN,4n}-(k_8\delta\tilde{T}_{LN,8e}+\mu_{4n}^i)T_{LN,4n}^i,\end{aligned} \tag{33}$$

$$\frac{dT_{LN,4e}^i}{dt} =\varphi(1-p)\gamma_4T_{LN,4n}^i+k_V(1-R_{LN}^{RT})\frac{V_{LN}}{c_2+V_{LN}}T_{LN,4e}-(k_8\tilde{T}_{LN,8e}+\mu_{4e}^i)T_{LN,4e}^i, \tag{34}$$

$$\frac{d\tilde{T}_{LN,8n}}{dt} =v(1-f)s+(1-\varphi)R\tilde{T}_{LN,8n}-\mu_{8n}\tilde{T}_{LN,8n}, \tag{35}$$

$$\frac{d\tilde{T}_{LN,8e}}{dt} =\varphi R\tilde{T}_{LN,8n}-\mu_{8e}\tilde{T}_{LN,8e}, \tag{36}$$

$$\frac{dT_{LN,8n}}{dt} =(1-v)(1-f)s+(1-\varphi)\gamma_8T_{LN,8n}-\mu_{8n}T_{LN,8n}, \tag{37}$$

$$\frac{dT_{LN,8e}}{dt} = \varphi\gamma_8 T_{LN,8n} - \mu_{8e}\tilde{T}_{LN,8e}, \tag{38}$$

$$\frac{dT_{LN,i}}{dt} = p(\gamma_4 T^i_{LN,4n} + \rho_{4n}\frac{V_{LN}}{c_2+V_{LN}}\tilde{T}^i_{LN,4n}) - (k_8\tilde{T}_{LN,8e} + \mu_1)T_{LN,i}, \tag{39}$$

$$\frac{dS_{LN,Ab}}{dt} = \rho_{Ab}(\tilde{T}^i_{LN,4e} + \tilde{T}_{LN,4e})\frac{V_{LN}}{c_2+V_{LN}} - k_{Ab}V_{LN}S_{LN,Ab} - \mu_{Ab}S_{LN,Ab}, \tag{40}$$

$$\frac{dM^a}{dt} = \frac{V_{LN}}{c_2+V_{LN}}(M - M^i - M^a) - \mu^a_M M^a + P_{LN}M^a_o, \tag{41}$$

$$\frac{dM^i}{dt} = k_{V,M}(1-R^{RT}_{LN})\frac{V_{LN}}{c_2+V_{LN}}(M - M^i) - \mu^i_M M^i + P_{LN}M^i_o - k_8\delta\tilde{T}_{LN,8e}M^i, \tag{42}$$

$$\begin{aligned}\frac{dV_{LN}}{dt} =& N_M M^i + N_T(\mu_i T_{LN,i} + \mu^i_{4e}\tilde{T}^i_{LN,4e} + \mu^i_{4e}T^i_{LN,4e}) - k_m\frac{V_{LN}}{c_2+V_{LN}}M^a \\ &- \frac{eV_{LN}}{c_1+V_{LN}}s - k_{V,M}(1-R^{RT}_{LN})\frac{V_{LN}}{c_2+V_{LN}}(M-M^i) \\ &- \overline{k_{V,M}}(1-R^{RT}_{LN})\frac{V_{LN}}{c_2+V_{LN}}20(N_{ICs}(1-\frac{t}{D_{FDC^i}}) - FDC^i) \\ &- k_V(1-R^{RT}_{LN})\frac{V_{LN}}{c_2+V_{LN}}(\tilde{T}_{LN,4n} + \tilde{T}_{LN,4e} + T_{LN,4n} + T_{LN,4e}) \\ &- k_{Ab}V_{LN}S_{LN,Ab} - \mu_V V_{LN} + R^V_{PB\to LV}V_{PB} - R^V_{LN\to PB}V_{LN},\end{aligned} \tag{43}$$

$$\frac{dFDC^i}{dt} = \overline{k_{V,M}}(1-R^{RT}_{LN})\frac{V_{LN}}{c_2+V_{LN}}(N_{ICs}(1-\frac{t}{D_{FDC^i}}) - FDC^i) - \mu^i_{FDC}FDC^i. \tag{44}$$

Equations (45) and (46) model the individual drug response level in the PB and LN, respectively. Those drug response levels are considered to be the drug effectiveness used in reducing the HIV-induced T4 cell infection.

$$\frac{dR^{RT}_{PB}}{dt} = K^{PB}_{in}(1 + \frac{E^{PB}_{max}C_c}{SC^{PB}_{50}+C_c} - K^{PB}_{out}R^{RT}_{PB}, \tag{45}$$

$$\frac{dR^{RT}_{LN}}{dt} = K^{LN}_{in}(1 + \frac{E^{LN}_{max}C_p}{SC^{LN}_{50}+C_p} - K^{LN}_{out}R^{RT}_{LN}. \tag{46}$$

According to the expressions (6) and (7), C_c and C_p denote the drug concentration expression in the PB and LNs, respectively.

Conflict of Interests

The authors declare that there is no conflict of interests.

Acknowledgments

This work was supported by the National Natural Science Fund of People's Republic of China (11271369).

REFERENCES

[1] WHO. Global summary of the AIDS epidemic 2013. http://www.who.int/hiv/data/epi_core_dec2014.png?ua=1 (accessed Nov 6, 2014).

[2] J. G. García-Lerma, et al., Oral pre-exposure prophylaxis for HIV prevention, Trends Pharmacol. Sci. 31 (2010), 74-81.

[3] M. S. Cohen, et al., Prevention of HIV-1 infection with early antiretroviral therapy, N. Engl. J. Med. 365 (2011), 493-505.

[4] Q. A. Karim, et al., Effectiveness and safety of tenofovir gel, an antiretroviral microbicide, for the prevention of HIV infection in women, Science 329 (2010), 1168-1174.

[5] VOICE (MTN-003) Microbicide Trials Network. http://www.mtnstopshiv.org/news/studies/mtn003 (accessed Nov 15, 2012).

[6] R. M. Grant, et al., Preexposure chemoprophylaxis for HIV prevention in men who have sex with men, N. Engl. J. Med. 363 (2010), 2587-2599.

[7] M. Thigpen, et al., Daily oral antiretroviral use for the prevention of HIV infection in heterosexually active young adults in Botswana: results from the TDF2 study. 6th IAS Conference; July 17-20, 2011. Rome, Italy. WELBC01 oral abstract. http://pag.ias2011.org/abstracts.aspx?aid=4631 (accessed Nov 15, 2012).

[8] J. Baeton, et al., Antiretroviral pre-exposure prophylaxis for HIV-1 prevention among heterosexual African men and women: The Partners PrEP Study. 6th IAS Conference; July 17-20, 2011. Rome, Italy. Abstract MOAX0106. http://pag.ias2011.org/flash.aspx?pid=886 (accessed Nov 15, 2012).

[9] FEMem-PrEP Project. FHI360. http://www.hi.org/en/Research/Projects/FEM-PrEP.htm (accessed Nov 28, 2011).

[10] J.M. Baeten, et al., Antiretroviral prophylaxis for HIV prevention in heterosexual men and women, N. Engl. J. Med. 367 (2012), 399-410.

[11] M. C. Thigpen, et al., Antiretroviral preexposure prophylaxis for heterosexual HIV transmission in Botswana. N. Engl. J. Med. 367 (2012), 423-434.

[12] L. V. Damme, et al., Preexposure prophylaxis for HIV infection among African women. N. Engl. J. Med. 367, 411-422 (2012).

[13] P. L. Anderson, et al., Emtricitabine-Tenofovir concentrations and pre-exposure prophylaxis efficacy in men who have sex with men. Sci. Transl. Med. 4,151ra125 (2012).

[14] WHO HIV/AIDS Programme. Guidance on couples HIV testing and counselling, including antiretroviral therapy for treatment and prevention in serodiscordant couples. http://www.who.int/hiv/pub/guidelines/9789241501972/en/ (accessed Nov 15, 2012).

[15] WHO. Prevention and treatment of HIV and other sexually transmitted infections among men who sex with men and transgender people. http://www.who.int/hiv/pub/guidelines/msm_guidelines2011/en/ (accessed Nov 15, 2012).

[16] D. Holmes, FDA paves the way for pre-exposure HIV prophylaxis. Lancet 380 (2012), 325.

[17] I. Cremin, et al., The new role of antiretrovirals in combination HIV prevention: a mathematical modelling analysis. AIDS 27 (2013), 447-458.

[18] V. Supervie, et al., Modeling dynamic interactions between pre-exposure prophylaxis interventions & treatment programs: predicting HIV transmission & resistance. Sci. Rep. 1, 185; DOI:10.1038/srep00185 (2011).

[19] E. De Clercq, Anti-HIV drugs: 25 compounds approved within 25 years after the discovery of HIV. Int. J. Antimicrob. Ag. 33 (2009), 307-320.

[20] A. Sharma, et al., Characteristics of indirect pharmacodynamic models and application to clinical drug responses. Br. J. Clin. Pharmacol. 45 (1998), 229-239.

[21] Q. Li, et al., Modeling of HIV-1 infection: insights to the role of monocytes/macrophages, latently infected T4 cells, and HAART regimes. PLoS ONE 7: e46026; DOI:10.1371/journal.pone.0046026 (2012).

[22] T. H. Finkel, et al., Apoptosis occurs predominantly in bystander cells and not in productively infected cells of HIV- and SIV-infected lymph nodes. Nat. Med. 1 (1995), 129-134.

[23] R. M. Granich, et al., Universal voluntary HIV testing with immediate antiretroviral therapy as a strategy for elimination of HIV transmission: a mathematical model. Lancet 373 (2009), 48-57.

[24] Drug Information Portal. Viread (Tenofovir Disoproxil Fumarate) - Description and Clinical Pharmacology. http://www.druglib.com/druginfo/viread/description_pharmacology/downloads/Viread(TenofovirDisoproxilFumarate)-DescriptionandClinicalPharmacology.pdf (accessed Nov 15, 2012).

[25] Gilead Sciences. Viread. http://www.gilead.ca/pdf/ca/viread_pm_english.pdf (accessed Nov 15, 2012).

[26] HIV Drug Interactions website. Tenofovir PK Fact Sheet. http://www.hiv-druginteractions.org/data/FactSheetImages/FactSheet_DrugID_221.pdf (accessed Nov 15, 2012).

[27] WHO. Guidance on pre-exposure oral prophylaxis (PrEP) for serodiscordant couples, men and transgender women who have sex with men at high risk of HIV: Recommendations for use in the context of demonstration projects. http://apps.who.int/iris/bitstream/10665/75188/1/9789241503884_eng.pdf (accessed Nov 15, 2012).

[28] G. Baheti, et al., Plasma and intracellular population pharmacokinetic analysis of tenofovir in HIV-1-infected patients. Antimicrob. Agents Ch. 55 (2011), 5294-5299.

[29] P. L. Anderson, et al., Pharmacological considerations for tenofovir and emtricitabineto prevent HIV infection. J. Antimicrob. Chemoth. 66 (2010), 240-250.